THEORETICAL MODELING OF BONDING CHARACTERISTICS AND PERFORMANCE OF WOOD COMPOSITES. PART II. RESIN DISTRIBUTION

Chunping Dai†
Senior Scientist and Group Leader

Changming Yu
Visiting Professor

Kevin Groves
Scientist
Forintek Canada Corp.
2665 East Mall
Vancouver, BC
Canada V6T 1W5

and

Hossein Lohrasebi
Postdoctoral Fellow
The University of British Columbia
No. 2900-2424 Main Mall
Vancouver, BC
Canada V6T 1Z4

(Received December 2005)

ABSTRACT

Further to the development of the inter-element contact model reported in Part I of this series (Dai et al 2006), this paper reports the development of a mathematical (analytical) model and a computer simulation (numerical) model of resin distribution. Based on theories of random coverage process and stochastic system, resin distribution is analytically defined by the average and the variance of resin coverage on constituent wood elements. To complement the analytical model, a numerical model using image digitization and Monte Carlo technique is developed on a computer to visualize and simulate the spatial variation of resin coverage. To validate the models, resin distributions on OSB strands are experimentally investigated using an image analysis technique. The analytical and numerical models are validated by close agreements with each other and with experimental results. It is proposed and modeled that resin coverage is classified into area coverage and mass coverage. The former follows an exponential relationship with resin content, while the latter has a linear relationship with resin content. Both area and mass coverage are strongly affected by element/strand thickness and wood density. The resin area coverage is further affected by resin spot thickness, density, and solids content. Resin spot size has no effect on the average but strong effect on the variance of resin coverage. Implications of the model predictions on improving uniformity and efficiency of resin application are also discussed.

Keywords: Wood composites, OSB, resin distribution, bonding, modeling, simulation.

INTRODUCTION

In the preceding paper of this series (Dai et al. 2006), a theoretical model and a computer simulation model were developed to predict the contact between constituent elements of wood composites during mat consolidation. To further predict bonding performance, one needs to characterize the resin distribution over the con-

† Member of SWST.

tacting element surfaces. Resin is probably the most adjustable and one of the most significant processing variables. It also represents a significant cost to wood composite manufacturing. Understanding the resin distribution is thus of great importance to not only optimizing product properties but also minimizing production costs.

Resin distribution has been a subject of several published studies, most of which were empirical (Burrows 1961; Meinecke and Klauditz 1962; Lehmann 1965 and 1970; Hill and Wilson 1978; Kasper and Chow 1980; Furno et al. 1983; Youngquist et al. 1987; Kamke et al. 1996; Smith 2003; Xie et al. 2004). The most significant work perhaps belongs to Meinecke and Klauditz (1962), who conducted a comprehensive study on the bonding physics and technology of particleboard. They conceptualized the structure of particleboard as a system of voids-dispersed wood particles and the bonding being related to the contact between particles and the strength of single adhesive joints. The adhesive joint strength was further governed by the continuity and uniformity of resin distribution. The results from their well-designed experiments showed that finer resin droplets and longer blending time led to more continuous and uniform resin distribution, and hence greater bonding strength. The similar effect of resin spot size was reported in several other studies (Burrows 1961, Hill and Wilson 1978; Lehmann 1965 and 1970; Kamke et al. 1996; Smith 2003). To quantify the resin distribution, various methods were developed using X-ray scanning (Kasper and Chow 1980; Xie et al. 2004) and image analysis (Youngquist et al. 1987; Kamke et al. 1996; Groves 1998).

While the above studies have provided general knowledge, the literature to date has yet to establish basic theories of resin distribution. More rigorous approaches are also needed to further understand the bonding mechanisms of wood composites. With the goal of developing a theoretical model for bonding, this paper has the following objectives:

- To analytically model and numerically simulate resin distribution,
- To experimentally evaluate resin distribution to validate the models, and
- To present typical predicted results of the characteristics of resin distribution and the effects of key processing variables.

MODELING AND SIMULATION

Similarly to Part I (Dai et al. 2006), the resin distribution is also investigated using both mathematical modeling and computer simulation. While the mathematical model offers analytical solutions, the computer simulation provides a powerful tool to consider real variables that may be too complex to be solved analytically.

Without losing generality, the constituent elements of wood composites are referred to as wood strands with defined length λ, width ω, and thickness τ. The resin distribution is defined in terms of *resin area coverage* R_a and *resin mass coverage* R_m. The area coverage R_a is the percentage of projected area of resin spots in a given area of strand surface. The mass coverage R_m is the solid resin mass per unit area of strand surface [g/m^2].

Theory and analytical modeling

Conceptualization and assumptions.—While the objective is to maximize resin coverage and disperse resin spots as uniformly as possible, the resin is normally applied in practice through a spraying process. During blending, the liquid resin is first atomized into streams of fine droplets. The resin droplets then make contact, in the spraying zone, with falling strands via a tumbling system (Meinecke and Klauditz 1962; Smith 2005). A massive number of resin droplets and strands are processed in a matter of seconds. Such a process can only generate a resin distribution that is random or at best uniformly-random. The spatial resin distribution over strand surfaces should follow, in theory, the law of the random coverage process. The random coverage theory (e.g. Hall 1988) offers a probabilistic description of random mechanism

governing the positioning and configuration of random flat sets (resin spots) in a two-dimensional plane (strand surface). Indeed, the distribution of resin spots on individual strands should depend on the random formation of resin droplets and the probability of strands passing through the spraying zone.

We thus model the resin distribution as a *random coverage process*. The following three general assumptions are made:

1) Resin spots are discs of uniform diameter, thickness, and density;
2) Resin spots are distributed independently of each other and in a uniformly-random manner, meaning that the probability of resin deposition over a given strand surface is independent and identical; and
3) Strand surfaces are dominated by those sided by strand length and width, with negligible edge surfaces.

Poisson resin coverage distribution.—Under Assumption 2, the resin coverage is mathematically described by the well-known Poisson process (e.g. Hall 1988). The Poisson distribution is suited for characterization of random events taking place with a very large number of trials and a very small probability of success. In a given blending process, the total number of trials (resin spots) N_r is enormous. Even the total number of resin spots per strand surface $N_{r,s}$ is very large. On the other hand, the probability of a single resin spot landing on a given strand area p_r is very small due to the small resin spot size in relation to the strand surface (Fig. 1). To be exact, the probability p_r is determined by the area ratio of resin spot over strand surface, or:

$$p_r = \frac{\frac{\pi}{4} d^2}{\lambda\omega} = \frac{\pi d^2}{4\lambda\omega} \tag{1}$$

where:
d = resin spot diameter [mm],
λ = strand length [mm], and
ω = strand width [mm].

When multiple resin spots are distributed, the calculation becomes more complex due to random overlaps between the resin spots (a resin droplet may strike a previously deposited resin spot, causing partial overlap). As shown in Fig. 1, some points on the strand surface are covered with more than one resin spot, while others are vacant. According to the Poisson coverage theory, the average number of resin coverage n_r equals the probability of single resin coverage p_r multiplied by the total number of resin spots $N_{r,s}$, or:

$$n_r = p_r N_{r,s} \tag{2}$$

Since there are two main surfaces per strand, the relationship between total number of resin spots per strand surface $N_{r,s}$ and that of a blend N_r is defined by:

$$N_{r,s} = \frac{N_r}{2N_f} \tag{3}$$

where: N_f = total number of flakes (or strands). Assuming no resin loss during blending, N_r is further determined by dividing the total mass of resin mix by that of a single resin droplet, or:

$$N_r = \frac{\frac{\lambda\omega\tau\rho_s N_f R_c}{(1+MC)R_{solids}}}{\frac{\pi}{4} d^2 \tau_r \rho_r} = \frac{4\lambda\omega\tau\rho_s N_f R_c}{(1+MC)\pi d^2 \tau_r \rho_r R_{solids}} \tag{4}$$

where:
τ, τ_r = thickness of strand and resin spot, respectively [mm],
ρ_s, ρ_r = density of wood strands and resin mix, respectively [kg/m^3],
MC = moisture content of wood strands,

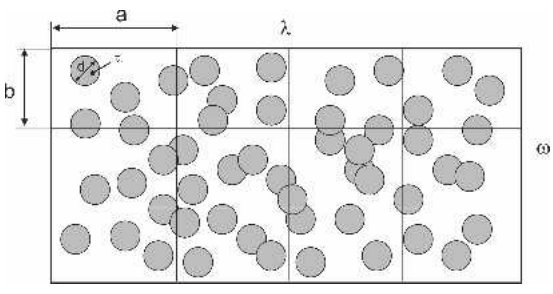

FIG. 1. Schematic of randomly-distributed resin spots on a strand surface (Note that resin spots are enlarged in relation to strand size).

R_c = resin content on oven-dry weight basis, and,

R_{solids} = resin solids content.

Combining Eqs. (1), (3) and (4), Eq. (2) becomes:

$$n_r = \frac{\tau \rho_s R_c}{2(1+MC)\tau_r \rho_r R_{solids}} \tag{5}$$

Equation (5) is the governing equation for calculating the average number of resin coverage at a given resin content, strand thickness, and wood density. In fact, this relationship holds regardless of resin distribution. Later we will discuss that Eq. (5), in fact, defines the *maximum* possible resin coverage under an *ideal* resin deposition process in which resin droplets repel each other and only strike vacant sites on strand surfaces, resulting in *no overlap* between spots. Obviously in a real resin deposition process, the spot overlap is inevitable and the local resin coverage is a random number. According to the Poisson distribution, the probability or percentage of a given strand surface area covered by *j* resin spots $p_r(j)$ is:

$$p_r(j) = \frac{a_j}{\lambda\omega} = \frac{e^{-n_r} n_r^j}{j!} \tag{6}$$

where: a_j = total area of a strand surface covered with *j* resin spots. The Poisson distribution is very simple to use because it is governed by only one parameter, i.e. its average and also variance n_r (Eq. 5).

Resin coverage and content relationships.—Of special interest concerning Eq. (6) is the case where *j* equals zero, i.e. no resin coverage. The probability or the percentage of a strand area containing no resin $p_r(0)$ is simply:

$$p_r(0) = \frac{e^{-n_r} n_r^0}{0!} = e^{-n_r} \tag{7}$$

Therefore, the resin area coverage R_a, which is the opposite of vacant area, is determined by:

$$R_a = 1 - p_r(0) = 1 - e^{-n_r} = 1 - \exp\left(-\frac{\tau \rho_s R_c}{2(1+MC)\tau_r \rho_r R_{solids}}\right) \tag{8}$$

where unity is the upper bound for R_a with R_c approaching infinity. Equation (8) analytically defines the relationship between resin coverage and resin content and how this relationship is affected by other variables. It reveals that the resin coverage R_a increases exponentially with strand thickness τ, strand wood density ρ_s, and resin content R_c, and decreases with resin spot thickness τ_r, density ρ_r, and resin solids content R_{solids}. The establishment of this relationship is essential to model bonding strength properties, since the bonding is more directly linked to the bonded area through the effect of resin coverage rather than resin content.

In comparison, the relationship between mass coverage R_m and resin content R_c is more straightforward. According to the definition and assuming no resin loss during blending, R_m equals the total resin mass per strand surface divided by the strand surface area, or:

$$R_m = \frac{\frac{\pi d^2}{4}\tau_r \frac{\rho_r}{R_{solids}} N_{r,s}}{\lambda\omega} = \frac{\pi d^2 \tau_r \rho_r N_{r,s}}{4\lambda\omega R_{solids}} \tag{9}$$

Also according to the definition, for a single strand, R_c is the total resin mass on two major surfaces divided by the strand mass (oven-dry basis), or:

$$R_c = \frac{2\frac{\pi d^2}{4}\tau_r \frac{\rho_r}{R_{solids}} N_{r,s}}{\frac{\lambda\omega\tau\rho_s}{1+MC}} = \frac{\pi d^2 \tau_r \rho_r N_{r,s}(1+MC)}{2\lambda\omega\tau\rho_s R_{solids}} \tag{10}$$

Combining Eqs. (9) and (10), a linear relationship between R_m and R_c can be readily obtained:

$$R_m = \frac{\tau \rho_s R_c}{2(1+MC)} \tag{11}$$

It is clear from Eq. (11) that strand thickness and density are the controlling factors in determining the resin mass coverage. Thicker or denser strands mean less surface area and therefore greater resin mass coverage.

Variability of resin coverage.—The uniformity of resin distribution can be evaluated in practice by the standard deviation or the vari-

ance of local resin coverage. At this stage, the analytical solution to calculating the variance of local area coverage is unknown. Here only the mass coverage variance is derived based on the spatial variability theory of stochastic systems (Ghosh 1951; Dodson 1971; Dai and Steiner 1997). The basic concept is that a resin spot of a certain size at a given point inevitably covers its neighboring points. Thus the local resin coverages are correlated from one point to another. Depending upon the spot diameter d and the distance between the points r, the autocorrelation function for uniformly-random resin distribution $\eta(r, d)$ is given by:

$$\eta(r,d) = \frac{2}{\pi}\left\{\cos^{-1}\left(\frac{r}{d}\right) - \frac{r}{d}\sqrt{1-\left(\frac{r}{d}\right)^2}\right\} \tag{12}$$

if $r < d$. Otherwise, $\eta(r, d)$ equals 0. Equation (12) suggests that the autocorrelation is in fact dependent upon the ratio of point-to-point distance and resin spot diameter.

Denote $\hat{R}_m$as the local averages of resin mass coverage [g/m^2]. Its variance $V(\hat{R}_m)$ [g^2/m^4] is given by:

$$V(\hat{R}_m) = \tau_r^2 \rho_r^2 n_r \int_0^{\sqrt{a^2+b^2}} \eta(r,d)p(r;a,b)dr \tag{13}$$

where function $p(r;a,b)$ is the distribution of random distances between two points within the rectangular sampling zone, and a and b are respectively zone length [mm] and width [mm] (Figs. 1 and 2). The random distance distribution was originally developed by Ghosh (1951) and applied for modeling mat formation by Dai and Steiner (1997). According to Eq. (13), the variance of resin mass coverage increases parabolically with resin spot thickness and density, and linearly with resin average coverage. It also increases, in a more complex manner, with an increase in resin spot size and a decrease in sampling zone size.

More details of the above derivations (Eqs. 12 and 13) are given in the appendix at the end of this paper.

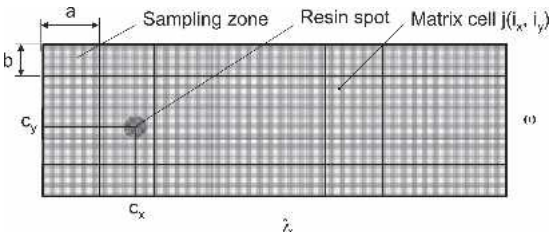

FIG. 2. Simulating resin distribution on a computer by digitizing the resin spot and the strand surface and sampling in segments.

Numerical modeling and computer simulation

A strand surface is digitized into pixels that can be described by a large matrix $j(i_x, i_y)$ (Fig. 2). While x and y define the two-dimensional coordinates, j indicates the number of resin disc overlaps, specifically, 0 meaning no resin coverage, and 1 or higher meaning one or multiple coverage. The program simulates the resin deposition process first by generating random number for center coordinates of resin spot c_x and c_y using the Monte Carlo technique. It updates the matrix $j(i_x, i_y)$ with each deposition of a droplet by adding one to or maintaining the previous cell values, depending upon whether or not the droplet falls on the location (i_x, i_y). After the deposition process, the program calculates the local and global averages as well as their variance or standard deviation.

The global average of resin area coverage $\overline{R}_a$ is calculated by adding the total areas of pixels covered with resin divided by strand surface area:

$$\overline{R}_a = \frac{s_p^2 \sum_{i_x=1}^{\lambda/s_p} \sum_{i_y=1}^{\omega/s_p} c(i_x,i_y)}{\lambda\omega} \tag{14}$$

where: s_p = side length of each pixel (e.g. 0.01 mm), and

$c(i_x, i_y)$ = resin coverage index which equals 1 if Pixel (i_x, i_y) is covered by resin or 0 if not.

The local averages of resin coverage $\hat{R}_a(I_x, I_y)$ are given by adding the total areas of pixels covered with resin within a sampling zone divided by zone area:

$$\hat{R}_a(I_x,I_y) = \frac{s_p^2 \sum_{i_x=(I_x-1)a+1}^{I_x a} \sum_{i_y=(I_y-1)b+1}^{I_y b} c(i_x,i_y)}{ab} \quad (15)$$

where: I_x and I_y = cell coordinates of sampling zone, and

a and b = side lengths of sampling zone (Fig. 2).

After obtaining the global and local averages, the variance of the local coverage averages $V(\hat{R}_a)$ is readily given by the following standard statistical relationship:

$$V(\hat{R}_a) = \frac{\sum_{I_x=1}^{\lambda/a} \sum_{I_y=1}^{\omega/b} (\hat{R}_a(I_x,I_y))^2}{(\lambda/a)(\omega/b)} - \overline{R}_a^2 \quad (16)$$

Likewise, the local averages and their variance of resin mass coverage can also be calculated. The global average of resin mass coverage $\overline{R}_m$ is calculated by:

$$\overline{R}_m = \frac{s_p^2 \tau_r \rho_r \sum_{i_x=1}^{\lambda/s_p} \sum_{i_y=1}^{\omega/s_p} j(i_x,i_y)}{\lambda\omega} \quad (17)$$

The local average of resin mass coverage $\hat{R}_m(I_x, I_y)$ is calculated by:

$$\hat{R}_m(I_x,I_y) = \frac{s_p^2 \tau_r \rho_r \sum_{i_x=(I_x-1)a+1}^{I_x a} \sum_{i_y=(I_y-1)b+1}^{I_y b} j(i_x,i_y)}{ab} \quad (18)$$

The variance of local resin content $V(\hat{R}_m)$ is calculated by:

$$V(\hat{R}_m) = \frac{\sum_{I_x=1}^{\lambda/a} \sum_{I_y=1}^{\omega/b} (\hat{R}_m(I_x,I_y))^2}{(\lambda/a)(\omega/b)} - \overline{R}_m^2 \quad (19)$$

EXPERIMENTAL

The purpose of the experimental tests was to determine the proper values of the input parameters for the models and to validate the model predictions. The blending tests of phenol-formaldehyde (PF) resin and commercial aspen strands were conducted using an 8-ft diameter OSB strand blender. The resin distributions were analyzed using an image analysis system.

Image analysis system

A camera system was developed at Forintek Canada Corp. to analyze the resin distributions on OSB strands (Groves 1998 and 2000). GluScan consists of a camera system, a PC, and image analysis software. Figure 3 shows the various components of the camera system, which includes: sample holder, fluorescent lighting, color video camera, and camera stand. The color video camera scans the surfaces of sample strands and then sends the data to a computer to automatically measure the following resin distribution features:

a) total resin coverage (% of image area covered by resin),
b) average resin spot diameter (micro) and area (micron^2), and
c) total number of resin spots per image (spots/image).

To recognize resin, GluScan relies on the color contrast between resin and background wood. Prior to measurement, the strands with PF resin need to be heated in an oven to cure the resin, giving it a distinctive dark red color, while strands with MDI resin need to be either tagged with a dye or sprayed with a chemical reagent to observe the resin.

With appropriate contrast, the imaging software can distinguish between the color of stained or cured resin and the lighter color of wood. If the wood is too dark and/or the resin is not cured or stained properly, the system cannot be used. Most commonly used OSB species work well with GluScan. The detailed description of GluScan can be found in relevant reports elsewhere (Groves 1998 and 2000).

Resin blending tests

Commercial aspen strands were air-dried, screened, and the geometry of approximately

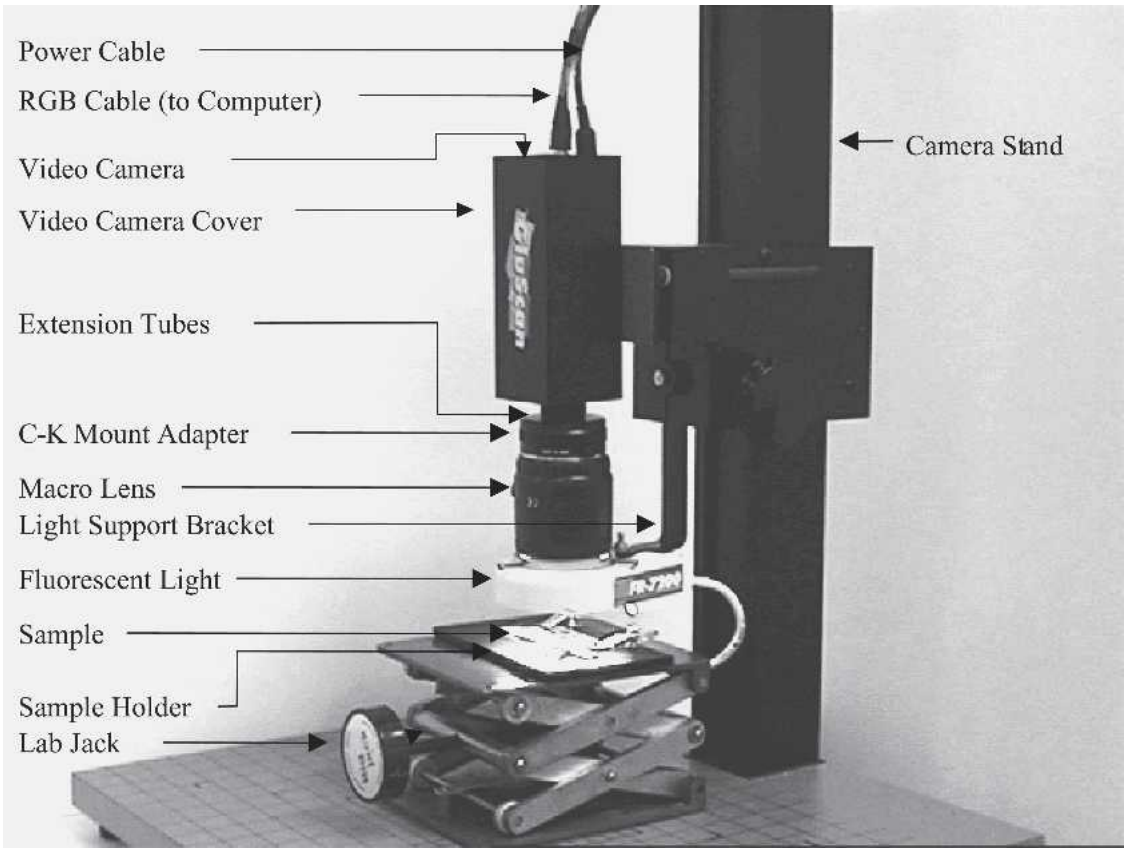

FIG. 3. Forintek's GluScan camera system for measuring resin distribution on OSB strands (Groves 1998).

2500 strands was determined. A total of 30 kg of strands was blended with a fixed 1% (w/w) wax (Cascowax EW-58S, 58% w/w solids content) and various levels of PF resin (Cascophen LP02/ Borden Chemical, 55% w/w solids content). The blender and the atomizer were run at 22.2 rpm and 16000 rpm, respectively. The strands were blended on the same batch sequentially with 7 different levels of phenol-formaldehyde (PF) resin: 2%, 3%, 4.5%, 6%, 7.5%, 9%, and 18% (all w/w) solids-based PF resin.

After each stage of adding PF resin, 0.5 kg of resinated strands was retrieved, from which 100 resinated strands were randomly selected and heated on wire racks in an oven at 175°C for 20 min for GluScan image analysis. After calibrating the camera system, five images were taken from each surface of the cooked strands, each image being from an area of 9.1 mm^2 (3.5 mm × 2.6 mm). A total of 1000 images per condition were analyzed for resin area coverage (%), spot diameter (micron), and spot area ($micron^2$).

RESULTS AND DISCUSSION

Model validations and implications

Model input parameters.—Table 1 lists the estimated resin spot size, spot thickness, resin density, strand density and thickness. These are the basic input parameters that the models require to predict the resin distribution. Although the average resin spot size is very small, the standard deviation (STD) is abnormally high. A better parameter for indicating the spot size variability might be the coefficient of variation (ratio of STD to average, or COV). Here the COVs are up to 290%, which is extremely high compared

TABLE 1. *Experimental data concerning resin distribution and strand dimensions.*

	Resin area coverage (%)					Spot diameter (micron)				
Resin content (%)	Average	STD	COV	Min	Max	Average	STD	COV	Min	Max
2	18.3	14	0.8	2	74	51.9	143	2.8	2.6	1205
3	26	15	0.6	2	86	58.5	162	2.8	2.6	1248
4.5	27.6	16	0.6	4	86	61.7	169	2.7	5.5	1229
6	45.6	14	0.3	11	95	72.6	189	2.6	5.7	1123
7.5	51.7	16	0.3	11	95	69.4	199	2.9	5.7	1120
9	52.6	14	0.3	14	92	70.7	198	2.8	5.7	1144
18	74.3	10	0.1	8	98	—	—	—	—	—
				Other Properties of PF Resin						
Density	1200 kg/m^3									
Spot Thickness*	0.02 mm									
				Strand Dimensions (mm)						
Length	77.3	24.2								
Width	16.8	11.6								
Thickness	0.65	0.18								

* Estimated by fitting data to Eq. (8)

to a 20% of a normally distributed variable. Indeed as shown in Table 1, the small averages result from mixes of very large and very small spots. This reflected how nonuniformly the resin was atomized by the spinning discs during blending. The spot thickness was estimated by fitting the experimental resin coverage with Eq. (8). In doing so, parameter τ_r partially becomes a "fudge" factor, which allows for consideration of such indefinable factors as resin transfer due to inter-strand rubbing and resin loss during blending. Here the spot thickness was that of liquid resin before pressing and curing. It should be noted that our models do not take into account the effect of pressing on lateral resin flow and hence coverage. Data concerning such an effect appear to be lacking in the literature. The consideration of press-induced resin flow would likely lead to slightly greater resin coverage in the finished panels than the model predictions.

Spatial distributions.—To help appreciate its random nature, the spatial resin distributions are visualized by an image of a real resinated strand (Fig. 4a) and the computer simulation (Fig. 4b). The simulation appears to be very similar to the real image in showing the discontinuous and chaotic resin distribution. The resin area coverage varies considerably from one location to another. The spatial correlation between the local coverages is governed by the distance separating the locations and the size of resin spots. Quantification of the resin distribution has been traditionally relied upon the use of image analysis methods (e.g. Youngquist et al. 1987; Kamke et al. 1996; Groves 1998). Here the computer simulation method is powerful not only for the purpose of visualization, but also for quantification of the resin distribution (Eqs. 14–19).

Relationship between area coverage and resin content.—This relationship defines one of the most essential characteristics of resin applica-

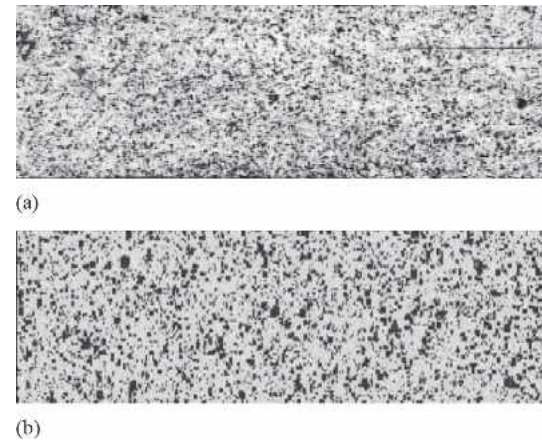

FIG. 4. Visualizing resin distribution: the spatial distribution of resin spots on a strand surface from: a) image analysis, and b) computer simulation.

tion, because bonding between strands is affected by resin content only through its effect on resin coverage (Meinecke and Klauditz 1962). To optimize performance and minimize cost, the resin coverage should always be maximized at a given resin content. Figure 5 depicts the relationships between resin area coverage and resin content under ideal and realistic conditions. Maximum resin coverage can be achieved in an *ideal* case where resin spots are distributed in an *ordered* manner with *no overlapping*. The relationship between maximum resin area coverage and content is linear, according to Eq. (5). A similar relationship was established by Meinecke and Klauditz (1962). In practice, however, overlaps between resin spots are inevitable due to the random distribution. As shown in Fig. 5, the measured resin area coverage follows a nonlinear relationship with resin content. According to Eq. (8), the relationship is in fact an exponential one. Indeed, close agreement can be found between the model predictions and the experimental observations.

The coverage appears to increase rapidly (almost linearly) with resin content when the resin usage is low. This is attributed to the fact that little or no overlap occurs when the total number of resin spots is low. Specifically, when the resin content is below 3%, the linear model seems to provide a good approximate solution. As the resin content increases, however, the discrepancy between the linear model and the exponential model widens simply because of the increased loss of resin coverage due to overlaps. Figure 5 shows that as much as 40% of resin coverage is lost at 11% resin content. From a physics standpoint, the overlaps may result from the natural *attraction* between the resin droplets. Therefore, any process (e.g. electrostatics, Groves 1997) that can generate *repulsion* between the resin droplets would help reduce the overlaps and therefore improve the resin efficiency. Moreover, the uniformity of resin distribution should also be improved once resin droplets repel each other. Finally, the model suggests that one can manipulate the resin coverage by adjusting such parameters as strand thickness and resin solids content.

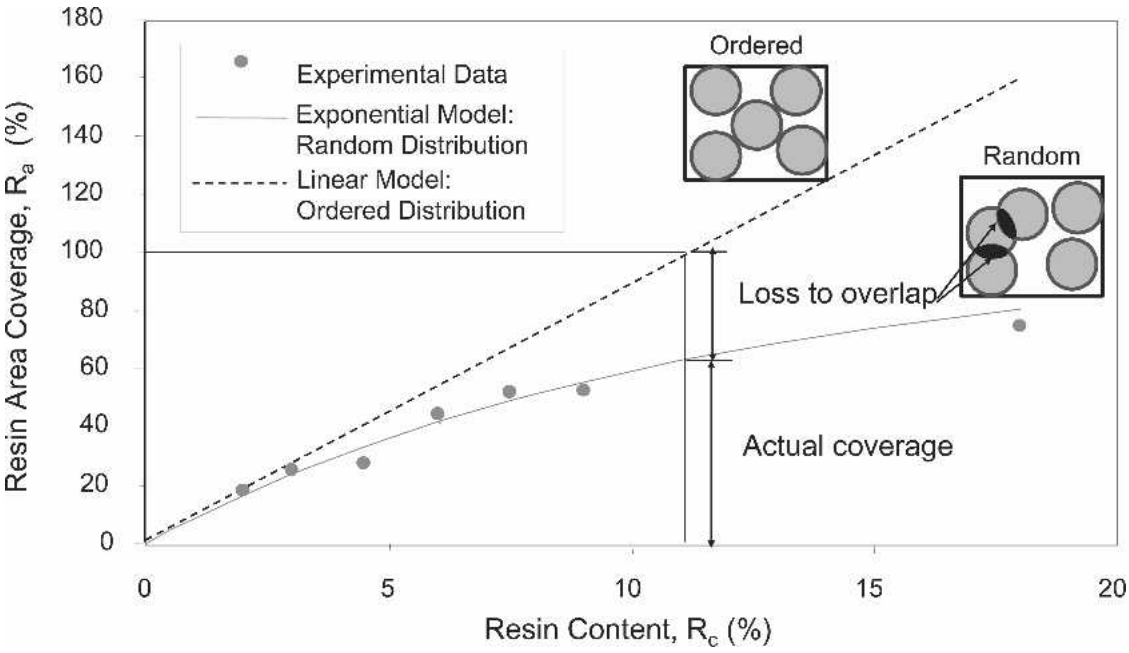

FIG. 5. Comparing resin area coverage between experimental data and model predictions, as well as random resin distribution and ordered distribution.

Variation of resin distribution.—Figure 6 compares the standard deviation (STD) of local resin mass coverage between the analytical model predictions (Eq. 13) and the computer simulations (Eq. 19) (note that standard deviation is the square root of variance). Again, very close agreement can be found, which mutually validates both the analytical and simulation models. According to the models, the mass STD is affected by many parameters including sampling zone size, resin spots and resin content. Figure 6 shows that the STD increases with resin content. This relationship is valid in many statistical systems where the variation increases with the average.

Contrary to resin mass coverage, however, the STD of resin area coverage is much different. As shown in Fig. 7, the area STD increases with resin content at low dosage levels. It reaches a maximum approximately at a resin content of 5% before slowly decreasing. Further increase in resin content leads to lower coverage STD or more uniformity. As one can imagine, the STD would approach zero if the resin content becomes extremely high. At this stage, the analytical form for calculating the coverage variation is unknown. However, the numerical solution via computer simulation is well defined (Eq. 16). This is a good example of the usefulness of numerical/computer simulation to handle complex problems.

While the simulation model predicted the trend well, Fig. 7 also reveals that a large difference existed between the predicted STD and the experimental data. The discrepancy likely comes from two sources: systematic variation from the blending process and variation of the resin spot size (Table 1). In developing the models, we assumed that the resin spots are uniform in diameter and *uniformly-random* in placement. Under these assumptions, the model predicted a *baseline* variation of resin coverage that appeared to be much lower than the real variation. This result implies that uniformly-random distribution may indeed represent the best uniformity and the real blending process is far from being uniformly random. How to achieve uniformly-random blending in practice would definitely be worthy of further investigation.

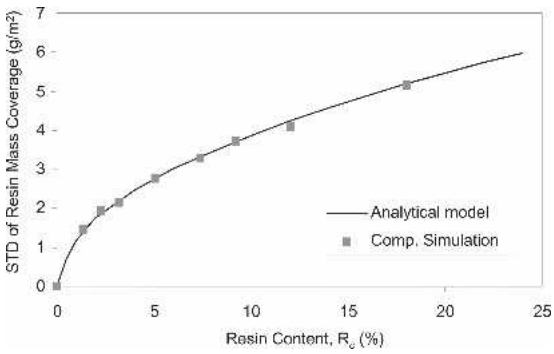

FIG. 6. Comparing standard deviation (*STD*) of resin mass coverage between the analytical model predictions and the computer model predictions.

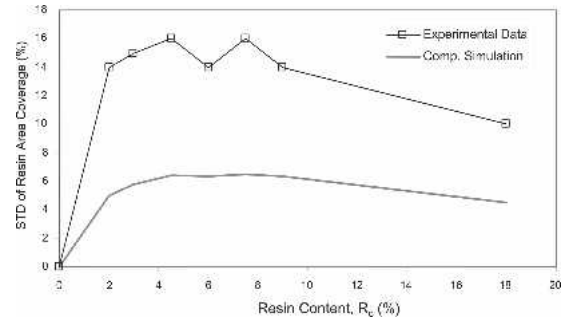

FIG. 7. Comparing standard deviation (*STD*) of resin area coverage between the computer simulation prediction and the experimental data.

Typical predicted results

Local resin coverage distribution.—Figure 8 depicts a family curve of the resin distributions at varying resin contents, based on the predictions from the simulation model. The model computed the local averages of resin area coverage in 3-mm × 3-mm-square zones (Eq. 15). The local coverage follows approximately the Poisson distribution, especially when the zone size is small and/or the resin content is low. More precisely, the Poisson distribution holds only when the zone size approaches zero. For bigger zones and/or higher resin contents, the distributions should become more symmetrical or closer to normal (Gaussian) distributions.

Resin area coverage vs mass coverage.—Fig-

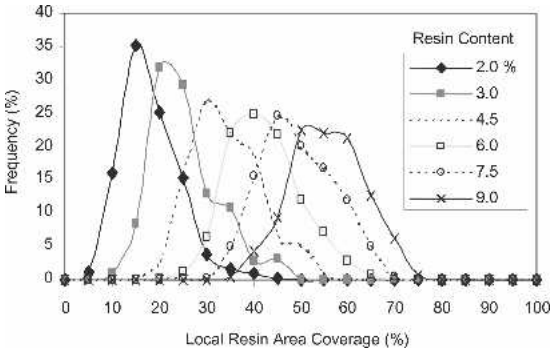

FIG. 8. A predicted family curve of local resin area coverage distributions at various resin contents.

ure 9 compares typical variations of resin area coverage and mass coverage with resin content. The former follows an exponential relationship (Eq. 8), while the latter is a linear relationship (Eq. 11). At lower resin content, there is little overlap between resin spots. Therefore, the area coverage increases rapidly with resin content. At higher resin content, resin spots start to overlap, leading to a slower growth rate of resin coverage. In comparison, the resin mass coverage always increases with resin content regardless of resin overlapping.

The differentiation between area and mass coverage may help reveal different bonding mechanisms between resin and wood elements. Investigations on the effect of resin area and mass coverage on bonding properties are underway. The results will be reported in our future publications.

Effect of strand thickness and density on resin coverage.—Strand thickness and density affect resin coverage through their effects on specific surface area. Thicker and/or denser strands have less surface area and therefore result in greater resin coverage than thinner and/or lower density strands at a given resin content. Such relationships were analytically defined by Eq. (8), and the typical predicted results are plotted in Figs. 10a and b. At lower resin content, the rate with which the resin coverage increases is also higher for the thicker strands (Fig. 10a) or denser wood species (Fig. 10b).

Other factors affecting resin area coverage include resin spot thickness, resin density, and solids content. According to Eq. (8), the area coverage can be significantly improved by reducing the resin spot thickness, density and solids content. By taking into account blending efficiency (resin loss), one may calibrate and use Eq. (8) to predict the quantitative improvement of resin coverage by modifying the resin mix and solids content.

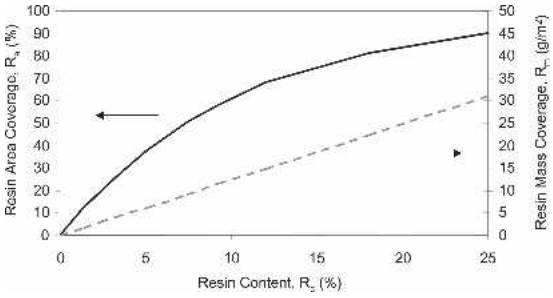

FIG. 9. Predicted resin area coverage and resin mass coverage as a function of resin content.

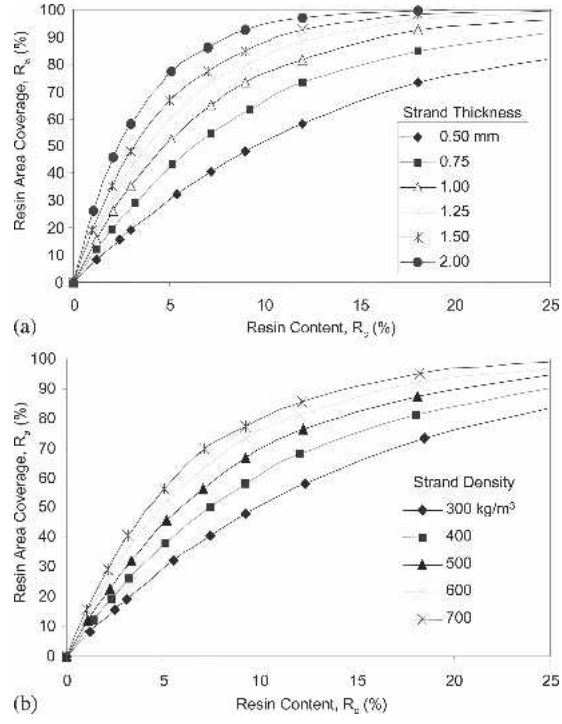

FIG. 10. Predicted effects of key processing variables on resin area coverage: a) Strand thickness, and b) Wood density.

It should be noted that Eqs. (8) and (11) were derived based on the assumption that strands are very thin and their edge surface areas are negligible compared to main face areas. Equations for calculating resin coverage for particles or fibers can be derived by considering a particle as being spherical or a fiber being cylindrical.

Effect of resin content and sampling zone size on resin coverage variation.—As shown in Figs. 11a and b, the STDs of resin mass coverage and area coverage are highly dependent upon the resin content and sampling zone size. As discussed earlier, an increase in resin content results in different responses in the variation of resin area coverage (Fig. 11a) and mass coverage (Fig. 11b). However, in both cases, larger sampling zone size always leads to smaller variation, simply due to a greater averaging effect. This result points to the random nature of resin distribution in terms of its relative uniformity on a large scale but great variability on a small scale. In practice, when using a camera to measure resin coverage, one must pay attention to the size of the inspection widow as it largely controls the outcomes of measured resin variability.

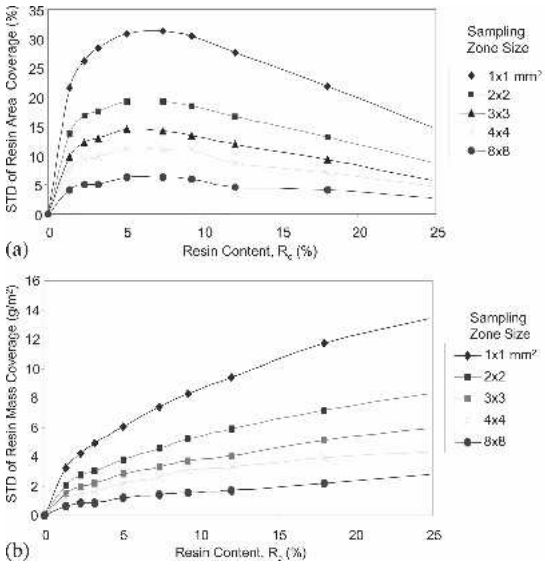

FIG. 11. Predicted effects of resin content and sampling zone size on: a) Standard deviation (*STD*) of resin area coverage, and b) Standard deviation (*STD*) of resin mass coverage.

Effect of resin spot size on resin distribution.—Figure 12 depicts the predicted increases of resin area coverage with resin content. Using the computer simulation model, we varied resin spot diameter from 0.04 mm to 0.64 mm and detected no effect on resin coverage. Indeed as shown by the analytical model (Eq. 8), resin spot size is a non-factor. This finding contradicts an earlier postulation that finer resin spots led to greater coverage (Meinecke and Klauditz 1962). Based on the computer simulation, the average resin coverage is independent of resin spot size as long as the resin is randomly distributed.

In contrast, the resin spot size has a significant effect on the variation of resin coverage. Figures 13a and b show the predicted baseline resin variation (STD), which is exclusive of systematic variation induced by the blending process. The STDs of resin area (Fig. 13a) and mass coverage (Fig. 13b) increase with resin spot size. Larger spot size means fewer resin spots for randomization. Moreover, a large spot covers a bigger area and therefore leads to stronger correlations between local coverages. As a result, larger resin spot size generates greater variation between local coverages. This finding is consistent with the general belief that small resin droplets are beneficial to improve resin coverage uniformity and hence bonding strength properties (Meinecke and Klauditz 1962; Burrows 1961; Hill and Wilson 1978; Lehmann 1965 and 1970; Kamke et al. 1996).

Better uniformity may not be the only reason why bonding properties improve with finer resin

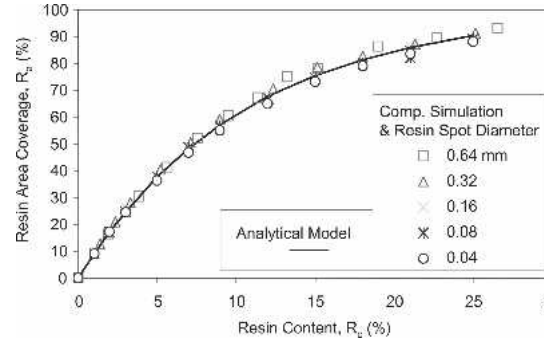

FIG. 12. Predicted effects of resin content and spot size on resin area coverage.

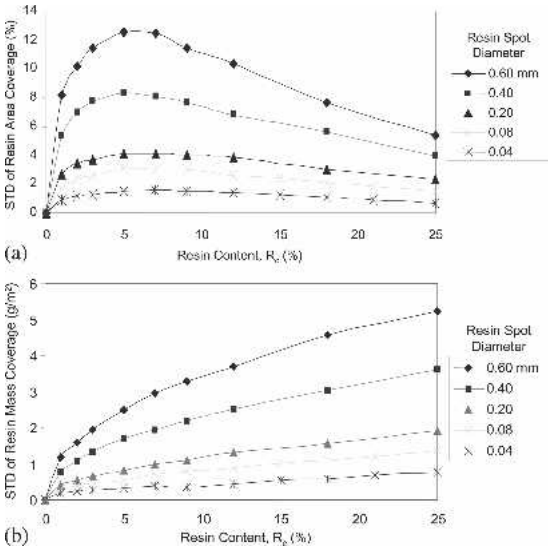

FIG. 13. Predicted effects of resin content and spot size on: a) Standard deviation (*STD*) of resin area coverage, and b) Standard deviation (*STD*) of resin mass coverage.

spot size. Closer distances between adjacent resin spots resulting from finer spot size may also be an important factor (Hill and Wilson 1978; Smith 2003). A model for predicting the distribution of distances between resin spots is nearly completed and will be published in a future paper.

SUMMARY AND CONCLUSIONS

Assuming uniformly-random dispersion of resin spots, analytical models and numerical/computer simulation models were developed for the first time to characterize resin distribution. The models predicted the average and the variance of resin coverages. Experimental investigations were also conducted to validate the models. The predictions from the analytical and computer simulation models agreed well with the experimental data. The following conclusions can be drawn from this study:

1. Resin distribution can be analytically predicted and numerically simulated. While the analytical models can provide theoretical understanding, the numerical models are powerful tools to simulate complex problems.
2. Resin coverages are differentiated by resin area coverage and mass coverage. The former has an exponential relationship with resin content, while the latter has a linear relationship with resin content.
3. The variability of resin area coverage is also different from that of resin mass coverage. The former peaks at a given resin content, whereas the latter monotonically increases with resin content.
4. Other variables affecting resin coverages are strand thickness and density due to their effect on strand surface areas. Resin spot thickness, resin density, and resin solids content also affect resin area coverage, but not mass coverage.
5. Resin spot size has no effect on the average resin area coverage, but a strong effect on the variation of local resin coverages because of their spatial correlation. Finer resin spots results in less variations in both area and mass coverage, and thus better uniformity.
6. Uniformity of the real resin distribution is significantly lower than that of uniformly-random resin distribution due to the systematic variation from the blending process and random variation of the resin spot size.

This paper has demonstrated the usefulness of theoretical and computer modeling for analyzing multiple variables involved in the resin application, which otherwise would be very difficult, if not impossible, to evaluate using experimental approaches. The proposed models may open a door for systematic analyses of the physics of blending process and the bonding mechanism of wood composites.

ACKNOWLEDGMENTS

Forintek Canada Corp. would like to thank its industry members, Natural Resources Canada, and the Provinces of British Columbia, Alberta, Quebec, Nova Scotia, New Brunswick, Saskatchewan, Newfoundland, and Labrador, for their guidance and financial support for this research. Funding from NSERC through a discovery grant is also gratefully acknowledged.

REFERENCES

BURROWS, C. H. 1961. Some factors affecting resin efficiency in flakeboard. Forest Prod. J. 11(1):27–3.

DAI, C., AND P. R. STEINER. 1997. On horizontal density variations in randomly-formed short-fibre wood composite boards. Composites Part A. 28(A):57–64.

——, C. YU, AND C. ZHOU. 2006. Theoretical modeling of bonding characteristics and performance of wood composites: Part I. Inter-element contact. Wood Fiber Sci. (in press).

DAI, C., AND P. R. STEINER. 1997. On horizontal density variations in randomly-formed short-fibre wood composite boards. Composites Part A. 28(A):57–64.

DODSON, C. T. J. 1971. Spatial variability and the theory of sampling in random fibrous networks. J. Roy. Statist. Soc. B. 33(1):88–94.

FURNO, T., C-Y. HSE WAND, AND W. A. CÔTÉ. 1983. Observation of microscopic factors affecting strength and dimensional properties of hardwood flakeboard. Pages 297–312 in T. M. Maloney, ed. Proc. 17th Washington State Univ. Inter. Particleboard/Composite Materials Symposium. Washington State Univ. Press, Pullman, WA.

GHOSH, B. 1951. Random distances within a rectangle and between two rectangles. Calcutta Math. Soc., 43:17–24.

GROVES, C. K. 1997. Assessment of new glue application technology for OSB. Technical Report. Forintek Canada Corp. 16 pp.

——, 1998. A new method for measuring resin distribution in OSB. Technical Report. Forintek Canada Corp. 58 pp.

——, 2000. The effects of resin distribution on oriented strand board properties. Technical Report. Forintek Canada Corp. 16 pp.

HALL, P. 1988. Introduction to the theory of coverage processes. John Wiley & Sons, New York, NY.

HILL, M. D. AND J. B. WITSON. 1978. Particleboard strength as affected by unequal resin distribution on different particle fractions. Forest Prod. J. 28(11):44–48.

KAMKE, F. A., E. KULTIKOVA, AND C. A. LENTH. 1996. OSB properties as affected by resin distribution. Pages 147–154 *in* Proc. Markets and Manufacturing in Panels/Composites for '96. The Fourth International Panel and Engineered-Wood Technology Conference & Exposition. Atlanta, GA.

KASPER, J. B., AND S. CHOW. 1980. Determination of resin distribution in flakeboard using X-ray spectrometry. Forest Prod. J. (30)7:37–40.

LEHMANN, W. F. 1965. Improved particleboard through better resin efficiency. Forest Prod. J. 15(4):155–161.

———. 1970. Resin efficiency in particleboard as influenced by density, atomization, and resin content. Forest Prod. J. 20(11):48–54.

MEINECKE, E., AND W. KLAUDITZ. 1962. Physics and technology of bonding in particle-board production. Research report of North Rhine Westfalia #1053. Westdeautscher Verlag, Colognne and Opladen (Translated from German by Israel Program for Scientific Translations in 1968). 81 pp.

SMITH, G. D. 2003. The lap-shear strength of droplets arrays of a PF-resin on OSB strands. Forest Prod. J. 53 (11/12): 1–7.

——, 2005. Direct observation of the tumbling of OSB strands in a industrial scale Coil blender. Wood Fiber Sci. 37(1):147–159.

XIE, Y., M. FENG, AND J. DENG. 2004. Quantification of UF and PF resins in MDF fiber with an X-ray fluorescence spectrometer. Wood Fiber Sci. 36(3):337–343.

YOUNGQUIST, J. A., G. C., MYERS, AND L. L. MURMANIS. 1987. Resin distribution in hardwood: evaluated by internal bond strength and fluorescence microscopy. Wood Fiber Sci. 19(2):215–224.

APPENDIX:

VARIATION OF LOCAL RESIN MASS COVERAGE

Point (maximum) variance.—Denote resin mass coverage at a given point $\dot{R}_m$[g/m^2]. For a single strand, the expected or average mass coverage $E(\dot{R}_m)$ equals the total mass of resin spots on one strand surface divided by the strand surface area, or :

$$E(\dot{R}_m) = \frac{\frac{\pi d^2}{4}\tau_r \rho_r N_{r,s}}{\lambda\omega} = \tau_r \rho_r E(j) \qquad (20)$$

where $E(j)$ is the expected or average overlap of resin spots, which is the same as n_r in Eq. (2). Equation (20) allows the relationship between the point mass coverage $\dot{R}_m$ and point overlap number j to be established:

$$\dot{R}_m = \tau_r \rho_r j \qquad (21)$$

Thus the variance of point mass coverage $V(\dot{R}_m)$ is given by:

$$V(\dot{R}_m) = \tau_r^2 \rho_r^2 V(j) = \tau_r^2 \rho_r^2 n_r \qquad (22)$$

where $V(j)$ is the variance of point resin overlap number which, by the nature of the Poisson distribution, equals its average n_r (Eq. 5). It represents the maximum theoretical variance of any sampling zone where the zone shrinks to a point. As the zone size increases, the variance will decrease because of the autocorrelation between points within the zone.

Autocorrelation.—Rewrite and organize the relationship between the point variance $V(j)$ and the average $E(j)$ as follows:

$$V(j) = E(j) = \frac{\pi d^2 N_{r,s}}{4\lambda\omega} = \frac{\pi d^2}{4}\gamma \qquad (23)$$

where γ is the number of resin spot per unit area or resin spot intensity: $N_{r,s}/\lambda\omega$. We can find that the resin disc area $\pi d^2/4$ in Eq. (23) is in fact the center locus of resin spots bound to cover a given point G (Fig. 14a). Thus, Eq. (23) implies that the variance of resin coverage at Point G, $V(j_G)$, equals the center locus of resin spots multiplied by the resin spot intensity. Likewise, the variance for coverage at two given points G and H, $V(j_{GH})$, should be governed by the product of the center locus of resin spots bound to cover both G and H, a_{GH}, and the spot intensity γ. As shown in Fig. 14b, it is not difficult to find that the locus area is determined by:

$$a_{GH} = 2\left(\frac{\theta d^2}{4} - \frac{dr\sin(\theta)}{4}\right) = \frac{\theta d^2}{2} - \frac{dr\sin(\theta)}{2} \qquad (24)$$

where θ is the angle between radius and Line GH, given by:

$$\theta = \cos^{-1}\left(\frac{r}{d}\right) \qquad (25)$$

Note also that r is the distance between G and H.

Thus the autocorrelation function is:

$$\eta(r,d) = \frac{V(j_{GH})}{V(j_G)} = \frac{a_{GH}\gamma}{\frac{\pi d^2}{4}\gamma} = \frac{2}{\pi d}(\theta d - r\sin\theta) \qquad (26)$$

Combining Eq. (25) with (26), we can get Eq. (12).

Variance of local averages.—Due to the autocorrelation, the variance of the local averages $V(\hat{R}_m)$ is always less than the point variance $V(\dot{R}_m)$. The relationship between the point variance and the local average variance is governed by:

$$V(\hat{R}_m) = \rho(a,b,d)V(\dot{R}_m) \qquad (27)$$

where $\rho(a,b,d)$ is the variance function, which is the weighted average of the autocorrelation function for all the points within the sampling zone of side lengths a and b, or:

$$\rho(a,b,d) = \int_0^{\sqrt{a^2+b^2}} \eta(r,d)p(r;a,b)dr \qquad (28)$$

Here $p(r; a, b)$ is the random distance function (Ghosh 1951; Dai and Steiner 1997). By combining Eq. (27) with Eqs. (28) and (22), we can get Eq. (13).

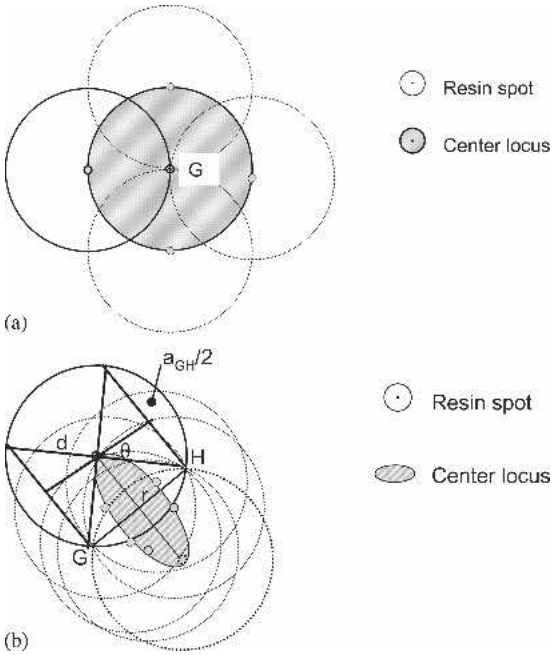

FIG. 14. Schematic of the center locus of a resin spot bound to cover: a) a given point G on strand surface, and b) two points G and H separated by a distance r.